

Life at the Energetic Edge: Kinetics of Circumneutral Iron Oxidation by Lithotrophic Iron-Oxidizing Bacteria Isolated from the Wetland-Plant Rhizosphere

Scott C. Neubauer,^{1*} David Emerson,² and J. Patrick Megonigal¹

Smithsonian Environmental Research Center, Edgewater, Maryland,¹ and American Type Culture Collection, Manassas, Virginia²

Received 1 March 2002/Accepted 7 May 2002

Batch cultures of a lithotrophic Fe(II)-oxidizing bacterium, strain BrT, isolated from the rhizosphere of a wetland plant, were grown in bioreactors and used to determine the significance of microbial Fe(II) oxidation at circumneutral pH and to identify abiotic variables that affect the partitioning between microbial oxidation and chemical oxidation. Strain BrT grew only in the presence of an Fe(II) source, with an average doubling time of 25 h. In one set of experiments, Fe(II) oxidation rates were measured before and after the cells were poisoned with sodium azide. These experiments indicated that strain BrT accounted for 18 to 53% of the total iron oxidation, and the average cellular growth yield was 0.70 g of CH₂O per mol of Fe(II) oxidized. In a second set of experiments, Fe(II) was constantly added to bioreactors inoculated with live cells, killed cells, or no cells. A statistical model fitted to the experimental data demonstrated that metabolic Fe(II) oxidation accounted for up to 62% of the total oxidation. The total Fe(II) oxidation rates in these experiments were strongly limited by the rate of Fe(II) delivery to the system and were also influenced by O₂ and total iron concentrations. Additionally, the model suggested that the microbes inhibited rates of abiotic Fe(II) oxidation, perhaps by binding Fe(II) to bacterial exopolymers. The net effect of strain BrT was to accelerate total oxidation rates by up to 18% compared to rates obtained with cell-free treatments. The results suggest that neutrophilic Fe(II)-oxidizing bacteria may compete for limited O₂ in the rhizosphere and therefore influence other wetland biogeochemical cycles.

Aerobic microorganisms that gain energy for growth from the oxidation of Fe(II) to Fe(III) at circumneutral pH face several daunting challenges. First, the energy available from Fe(II) oxidation is low [$\Delta G^{\circ} \approx 29$ kJ mol of iron⁻¹ for the reaction $\text{Fe(II)} + 0.25\text{O}_2 + \text{H}^+ \rightarrow \text{Fe(III)} + 0.5\text{H}_2\text{O}$ (7)]. Also, the half-life of Fe(II) in natural circumneutral freshwaters is approximately 2 to 10 min (depending on the pH) under air-saturated conditions (31), whereas the shortest reported doubling time for a lithotrophic Fe(II) oxidizer is about 8 h (10). These kinetic parameters limit circumneutral lithotrophic Fe(II) oxidizers to growth in microaerophilic zones at the interface between oxic and anoxic environments because abiotic Fe(II) oxidation rates are lower at lower O₂ concentrations (19, 31). The competition for Fe(II) in these environments is further enhanced by the fact that iron oxides and the surfaces of the microbes themselves can catalyze abiotic Fe oxidation. As a result, separating these interacting and competing mechanisms to determine the amount of Fe(II) that is actively oxidized (metabolized) by lithotrophic Fe(II) oxidizers is a real challenge.

The fact that organisms are able to successfully compete for Fe(II) is evident because of the abundant growth of lithotrophic Fe(II) oxidizers in oxic-anoxic boundary areas in a wide variety of circumneutral habitats (8, 14) where substantial concentrations of Fe(II) (>10 μM) are available. However, because there have been difficulties in obtaining pure cultures of

Fe(II) oxidizers from these environments, relatively little is known about the biology of Fe(II) oxidation at near-neutral pH values. *Gallionella ferruginea*, first described in the 19th century (6), is a lithoautotroph that can grow on Fe(II) as an energy source and CO₂ as a carbon source, although mixotrophic growth is possible in the presence of glucose (16). The physiology of *Leptothrix ochracea*, perhaps the most commonly recognized Fe(II) oxidizer due to its iron-encrusted sheaths and cell filaments, is even less understood due to a lack of pure cultures. Evidence suggests that this organism can grow in the presence of Fe(II) when there are no other major electron donors (12, 22). The development of gradient techniques for enrichment of circumneutral Fe(II) oxidizers besides *G. ferruginea* and *L. ochracea* has revealed that putatively lithotrophic Fe(II) oxidizers are widespread (14) in a variety of environments, including groundwater springs (10, 11, 14), freshwater and marine hydrothermal vents (5, 17), and wetlands (13, 28; J. V. Weiss, J. P. Megonigal, D. Emerson, and S. M. Backer, submitted for publication). To date, few detailed studies necessary to describe the biogeochemical significance of these organisms have been conducted.

Recently, lithotrophic Fe(II) oxidizers were enriched from the roots of wetland plants growing at circumneutral pH (13; Weiss et al., submitted). Theoretically, the rhizosphere is an ideal environment for microbial Fe(II) oxidation. Although O₂ diffusing from the atmosphere typically penetrates only several millimeters into the wetland soil surface, the oxic-anoxic interface in wetlands is extended by plant roots that leak oxygen via a process known as radial oxygen loss (1, 3). In wetland porewater containing dissolved Fe(II), radial oxygen loss promotes

* Corresponding author. Mailing address: Smithsonian Environmental Research Center, P.O. Box 28, Edgewater, MD 21037. Phone: (443) 482-2355. Fax: (443) 482-2380. E-mail: neubauer@serc.si.edu.

the formation of iron plaque on the roots (21). Due to the speed of Fe(II) oxidation in circumneutral environments, it has been presumed that most Fe plaque formation is due to abiotic Fe(II) oxidation. However, the presence of substantial numbers of Fe(II) oxidizers in the rhizosphere (~1 to 6% of the total microbial community [Weiss et al., submitted]) and the microaerophilic nature of the rhizosphere suggest that microbial Fe(II) oxidation may be significant. This study was designed to determine the potential role of microbial Fe(II) oxidation by using laboratory batch cultures of an organism enriched from the roots of a circumneutral wetland plant. A second objective was to identify abiotic variables that affect microbial Fe(II) oxidation. Although the batch system used could not replicate the inherent complexity of the rhizosphere, it did allow precise manipulation of important abiotic variables (e.g., pH, O₂, and temperature) that influence Fe(II) oxidation in all environments.

MATERIALS AND METHODS

Bacterial strains. All experiments described below in detail were conducted with a neutrophilic, lithotrophic, Fe(II)-oxidizing bacterium (strain BrT) isolated from the roots of *Typha latifolia* (broad-leaved cattail) growing in a constructed wetland on the Chesapeake Bay in Maryland. Gradient tubes with opposing gradients of O₂ and Fe(II) (as FeS) were used for the initial enrichment, for isolation, and for the subsequent maintenance of the culture (10; Weiss et al., submitted). Strain BrT is similar to strain CCJ, a neutrophilic Fe(II) oxidizer isolated from the roots of the soft rush, *Juncus effusus* (13); neither strain grows on heterotrophic medium, reduced sulfur compounds, Mn(II), H₂, or formate (all electron donors), nor can these strains use NO₃⁻ as an electron acceptor (13; J. V. Weiss, unpublished data). Strain BrT grows at circumneutral pH values (pH ~5.8 to 7.0) and at temperatures ranging from 18 to 37°C (Weiss, unpublished data). Analysis of the 16S small-subunit rRNA gene indicates that BrT is part of a novel lineage of γ -proteobacteria in the *Xanthomonas* group and is closely related to other neutrophilic Fe(II) oxidizers isolated from the wetland-plant rhizosphere (Weiss, unpublished data), groundwater (10), and marine hydrothermal vents (8). Details concerning the isolation and descriptions of BrT and other isolates of Fe(II) oxidizers will be published elsewhere. Three other lithotrophic Fe(II) oxidizers (LD-1, a freshwater strain isolated from the rhizosphere [Weiss, unpublished data], and JV-1 and PV-1, marine strains from Loihi Seamount in the Pacific Ocean [9]) were also used in some of our studies.

Bioreactor configuration. Batch cultures of cells (1.5 liters) were grown in a pair of bioreactors (Applikon, Madison, N.J.) coupled to microprocessor controllers that allowed precise manipulation of pH (± 0.1 pH unit), temperature ($\pm 0.1^\circ\text{C}$), and dissolved oxygen content ($\pm 0.2\%$ of air saturation). The pH was maintained by automatic additions of 1 N HCl and 500 mM NaHCO₃, temperature was maintained with a thermal jacket that encircled the bioreactors, and the dissolved oxygen content was controlled by bubbling filter-sterilized N₂ or air through the growth medium. During the experiments, the pH (pH 6.5) and the temperature (27.0°C) were kept constant. The O₂ setpoint was systematically varied between 0 and ~5% of air saturation throughout each experiment, and a series of Fe(II) oxidation measurements was made at each O₂ level (see below). In the bioreactors, cells were grown in a minimal freshwater medium (18.7 mM NH₄Cl, 0.8 mM MgSO₄ · 7H₂O, 0.7 mM CaCl₂ · 2H₂O, 0.3 mM K₂HPO₄) supplemented with trace minerals and vitamins (10). The marine strains (JV-1 and PV-1) were grown in an artificial seawater medium (9); all of the other conditions were the same. The medium was amended with 5 or 10 mM NaHCO₃ to buffer the pH and to provide an inorganic carbon source for the putatively lithotrophic Fe(II) oxidizers.

Each bioreactor was inoculated with a 1 to 2% inoculum of either (i) live Fe(II) oxidizer cells, (ii) Fe(II) oxidizer cells killed with sodium azide (final azide concentration, 1 mM; azide added immediately or several days after inoculation), or (iii) abiotic Fe(III) oxides (no cells) from sterile gradient tubes. The inocula with cells also contained Fe(III) oxides because it was not possible to separate the cells from oxides produced during cell growth without damaging the cells. During the initial experiments, the bioreactors (regardless of inoculum type) were fed by addition of 84 to 212 μmol of FeCl₂ · 4H₂O every 4 h over a period of 24 min. Under this feeding regimen, the dissolved Fe(II) concentrations fluctuated widely between FeCl₂ additions. Therefore, to avoid Fe(II) limitation

of cell growth, a second set of experiments was conducted with FeCl₂ · 4H₂O added continuously with a peristaltic pump to the bioreactors at rates of 12 to 3,000 $\mu\text{mol h}^{-1}$. In this continuous-feeding mode, the Fe(II) addition rates were manually adjusted to prevent excess accumulation or depletion of Fe(II) in the bioreactors. The typical dissolved Fe(II) concentrations were 10 to 100 μM , and the range was 0 to >1,500 μM .

Fe(II) oxidation rate measurements. For a subset of the bioreactor runs, Fe(II) oxidation rates were measured following addition of a single, relatively large Fe(II) pulse. A sterile solution of ferrous iron (as FeCl₂ · 4H₂O) was added with a syringe to each bioreactor to raise the Fe(II) concentration by ~300 to 900 μM . The disappearance of Fe(II) was monitored by collecting samples at 10- to 30-min intervals for several hours and measuring Fe(II) concentrations with ferrozine as described below. The rate of Fe(II) oxidation was calculated by determining the slope of [Fe(II)] versus time. When Fe(II) was continuously added to the bioreactors, oxidation rates were calculated by determining the difference between the expected rate of change in the Fe(II) concentration in the absence of oxidation [i.e., the Fe(II) addition rate] (micromolar per hour) and the observed rate of change in the Fe(II) concentration within the bioreactor (micromolar per hour). The Fe(II) addition rate was calculated as a function of the concentration and volume of Fe(II) added to the bioreactors and the volume of medium in each bioreactor. Typically, for each continuous-feeding experiment, at least two rate measurements were obtained at each Fe(II) addition rate.

Chemical and microbiological analyses. Dissolved Fe(II) concentrations were measured spectrophotometrically at 562 nm after an aliquot of a filtered (pore size, 0.22 μm) sample from a bioreactor was added to 0.1% ferrozine in 50 mM HEPES buffer (20). The total Fe concentrations [including the concentrations of dissolved Fe(II), particulate Fe(III) oxides, and Fe(II) adsorbed to the oxides] were measured in unfiltered samples by using ferrozine after reduction of all iron to Fe(II) in a 0.25 M hydroxylamine hydrochloride solution in 0.25 M HCl that was incubated on a shaker table (150 rpm) for at least 2 h (11). The median standard deviation for duplicate FeCl₂ · 4H₂O standards in the concentration range from 0 to 1,000 μM was ± 2 μM . Cell density was determined after duplicate 10- μl samples were spread on agar-coated slides inscribed with 1-cm-diameter circles (fluorescent antibody slides; Gold Seal Products, Highland Park, Ill.) (9). When these samples were dry, they were stained with 10 μl of 250 μM SYTO 13 (a nucleic acid-specific stain; Molecular Probes Inc., Eugene, Oreg.) and counted under epifluorescence conditions by using a 100 \times objective lens on an Olympus BX 60 microscope. A minimum of 15 fields or 400 cells was counted per sample. To determine the protein content of strain BrT, it was grown to the late log phase in gradient tubes. The cells were concentrated by centrifugation, and the resulting cell pellet was treated with 0.5 M hydroxylamine-HCl for 30 min at 35°C to remove Fe(III). The low-melting-point agarose remaining with the cell pellet was removed by heating the cell suspension at 70°C for 20 min, immediately centrifuging it, and discarding the supernatant. The remaining cell pellet (approximately 25 μl) was frozen (plunged in liquid N₂) and thawed (placed in a heating block at 70°C for 30 s) eight times to lyse the cells. The total protein content was then determined with a protein assay kit (Bio-Rad Laboratories, Hercules, Calif.) based on the Bradford method, with bovine gamma globulin as the protein standard.

Data analysis and calculations. Ferrous iron oxidation rates can potentially be influenced by pH, temperature, the concentrations of dissolved O₂, Fe(II), and Fe(III), the Fe(II) supply rate, and the number of Fe(II)-oxidizing bacteria (19, 25, 31, 32, 33). Furthermore, bacteria may influence Fe(II) oxidation kinetics directly by actively metabolizing Fe(II) or indirectly by either accelerating or inhibiting abiotic oxidation rates. Multiple linear regression models were used to determine the effects of these variables on Fe(II) oxidation rates (r) [expressed as micromolar Fe(II) oxidized per hour]:

$$r = (v_1 \times m_1) + (v_2 \times m_2) + \dots + (v_n \times m_n) + b \quad (1)$$

where m_1 to m_n are slope coefficients for variables v_1 to v_n (e.g., pH, [Fe]_{total}, O₂) and b is the intercept of the regression. Data from all continuous-feeding experiments were pooled by treatment (>50 rate measurements per treatment) and used to calculate separate slope and intercept coefficients for bioreactors with live, killed, and no cells. Because coincident measurements of cell density and Fe(II) oxidation rates were available for only a small subset of all samples ($n = 9$), cell density was not included in the stepwise multiple linear regression analysis. The final regression equations included only those variables that were significant in all three treatments ($P < 0.05$). The propagation of standard deviations for each slope coefficient and intercept produced error estimates for the calculated oxidation rates (26). All regression analyses were conducted by using SAS v.8.1 (SAS/STAT user's guide, version 8; SAS Institute, Cary, N.C.).

Under identical conditions (e.g., identical pH, O₂, and [Fe]_{total} conditions), the

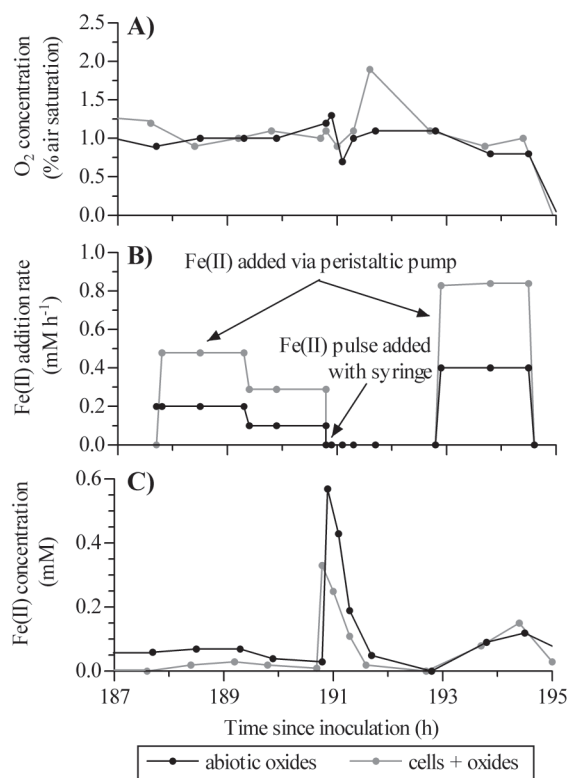


FIG. 1. Sample raw data collected during the continuous-feeding experiments for paired bioreactors inoculated with cells or abiotic oxides. Data are from the run started on 9 May 2001. (A) Dissolved oxygen concentrations. (B) Rate of continuous Fe(II) addition. When Fe(II) pulses were added by syringe, the continuous-feed Fe(II) pumps were turned off. (C) Dissolved Fe(II) concentrations. Note that higher rates of Fe(II) addition to the live-cell bioreactor did not typically result in higher Fe(II) concentrations.

difference in modeled oxidation rates between the live-cell and killed-cell treatments is a measure of active bacterial Fe(II) metabolism (i.e., biotic oxidation rate = $r_{\text{live cells}} - r_{\text{killed cells}}$). A comparison of the killed-cell and no-cell treatments indicates any secondary bacterial effects on abiotic oxidation rates due to the presence of cells or cell products (e.g., exopolymers) in the growth medium (i.e., secondary cellular effects = $r_{\text{killed cells}} - r_{\text{no cells}}$). Our data could not quantify how competition for O_2 by live Fe(II) oxidizers influenced abiotic Fe(II) oxidation rates. Negative secondary effects (i.e., $r_{\text{killed cells}} < r_{\text{no cells}}$) implied that the bacterial cells or cellular by-products inhibited abiotic Fe(II) oxidation. The net effect of the bacteria on total Fe(II) oxidation rates was the sum of biotic oxidation and secondary cellular effects (i.e., net effect = $r_{\text{live}} - r_{\text{no cells}}$). Thus, if the cells actively metabolized Fe(II) but simultaneously depressed chemical oxidation rates by the same amount, there would be no net change in the total Fe(II) oxidation rate.

RESULTS

Bioreactor operation and performance. Over the course of a bioreactor run, we systematically and independently varied the O_2 concentrations and Fe(II) addition rates so that the effects of these variables on Fe(II) oxidation rates could be determined. The dissolved oxygen levels were normally stable (e.g., the levels at <190 h in Fig. 1A). However, when the O_2 set-point or Fe(II) addition rate was changed, the O_2 concentrations were more variable (e.g., the concentrations at 191 to 192 h in Fig. 1A) and required a lag period before they stabi-

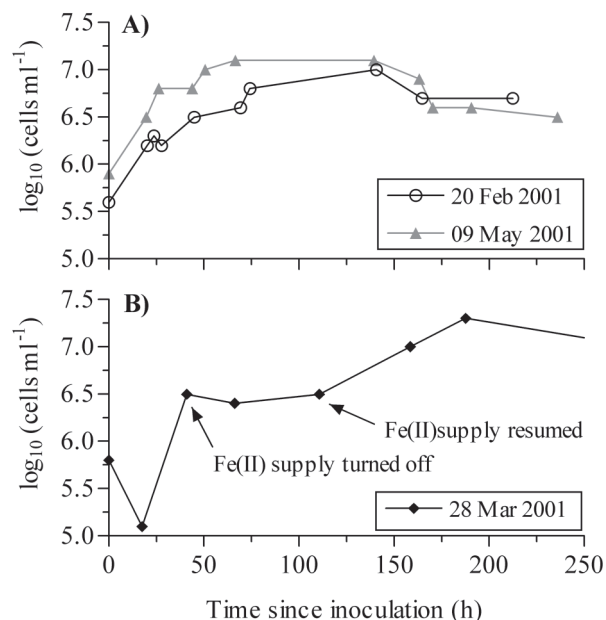


FIG. 2. Sample growth curves for BrT. The dates are the inoculation dates for the bioreactor runs. (A) Typical growth curves from several bioreactor runs. (B) Effect of Fe(II) supply on cell growth. Cell density did not increase in the absence of an Fe(II) supply.

lized. To maintain dissolved Fe(II) concentrations in the range from approximately 50 to 150 μM , the Fe(II) addition rate was manually adjusted after each sampling interval (Fig. 1B). Periodically, the Fe(II) addition rates were systematically varied to provide a wide range of addition rates at similar O_2 and total Fe levels. Because Fe(II) oxidation rates were generally higher in bioreactors inoculated with live BrT cells (see below), these bioreactors usually required a higher Fe(II) addition rate to maintain the target Fe(II) concentration. As a result, the total Fe concentrations in paired bioreactors (i.e., bioreactors started on the same day) differed during the course of a bioreactor run. Despite variability in the Fe(II) addition rates and the concentrations of O_2 and total Fe, the dissolved Fe(II) concentrations for paired bioreactors were generally comparable [i.e., the range of Fe(II) concentrations for the bioreactors was <100 μM] (Fig. 1C).

Cell growth. Following inoculation of the bioreactors, the initial cell densities of BrT ranged from 4.8×10^4 to 1.1×10^6 cells ml^{-1} . During our initial experiments, when the bioreactors were stirred at an impeller rate of 300 rpm, cell growth was very poor. When the stirring rate was lowered to 150 rpm, the cells grew more consistently. Growth curves representative of successful bioreactor runs are shown in Fig. 2A. With FeCl_2 as an Fe(II) source, the doubling times ranged from approximately 17 to 33 h (mean, 25 h) (Table 1). The maximum cell yields for BrT ranged from 9.8×10^6 to 1.8×10^7 cells ml^{-1} (Table 1). The average cell protein content was 1.3×10^{-14} g of protein cell^{-1} (or 1.2×10^{-14} g of C cell^{-1} , assuming that protein and carbon account for 55 and 50% of the dry cell biomass, respectively). There were no significant correlations between initial or maximum cell density and doubling times ($P > 0.17$). The doubling times for BrT were comparable to those

for other strains of Fe(II) oxidizers grown in the bioreactors under similar conditions (data not shown). After the maximum cell density was reached, the sizes of the populations of BrT cells gradually declined until the termination of each experiment (Fig. 2A).

On one occasion, the FeCl₂ supply to the bioreactor was shut off for approximately 3 days during the log growth phase. In the absence of an Fe(II) supply, BrT showed no growth (Fig. 2B). Following the resumption of delivery of FeCl₂ to the bioreactor, the cell density increased from 3.2×10^6 cells ml⁻¹ to a maximum of 1.8×10^7 cells ml⁻¹. The doubling time for growth after the Fe(II) supply was restored was approximately 30.5 h (Table 1). The growth of another rhizosphere iron oxidizer (strain LD-1) and the growth of a marine hydrothermal vent strain (PV-1) also ceased when the Fe(II) supply to the bioreactor was stopped (data not shown). Strain PV-1 resumed growth when the FeCl₂ supply was restored, whereas LD-1 did not show additional cell growth.

Oxidation rates in pulse-feeding mode. Pulsed additions of FeCl₂ to the bioreactors raised final dissolved Fe(II) levels to 300 to 900 μM. Regardless of the starting Fe(II) concentration, the rates of Fe(II) disappearance were linear down to ~100 μM (typical r^2 , >0.95) (Fig. 3). The oxidation rates decreased below this level, suggesting that oxidation had become Fe(II) limited. Therefore, oxidation rates were calculated by using data points where the dissolved Fe(II) concentrations were more than 100 μM. The measured oxidation rates in the bioreactors ranged from 26 to >1,000 μM h⁻¹ and were significantly described ($r^2 > 0.82$; $P < 0.001$) by the heterogeneous rate equation:

$$-d[\text{Fe(II)}]/dt = \{k_1 + k_2 \times [\text{Fe(III)}]\} \times [\text{Fe(II)}] \quad (2)$$

where k_1 is the homogeneous rate constant (time⁻¹) and k_2 is the heterogeneous rate constant (molar⁻¹ time⁻¹). k_1 and k_2 were calculated as functions of [O₂] and pH using previously described equations (32). Using these equations to calculate k_1 and k_2 (32) resulted in calculated oxidation rates that were ~60% of measured values, suggesting that the kinetics of iron oxidation in the bioreactors and the kinetics of iron oxidation in a strictly abiotic system are different. The Fe(II) disappearance rates at 0% O₂ saturation [an estimate of Fe(II) sorption to particles] were low in both pulse- and continuous-feeding modes (the average was 34 μM h⁻¹ for a range of [Fe]_{total}; $n = 9$) and were positively and linearly correlated with [Fe]_{total} ($r^2 = 0.87$; $P < 0.001$) (data not shown).

To directly determine the fraction of total Fe(II) oxidation due to bacterial metabolism, consecutive Fe(II) pulses were

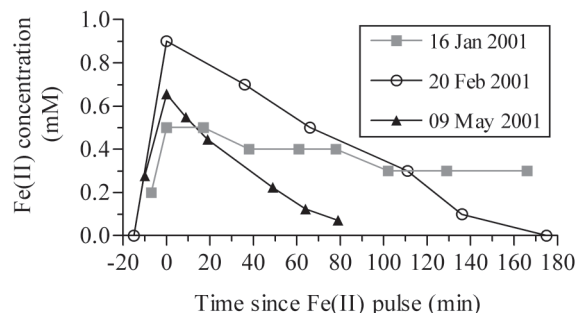


FIG. 3. Sample plots of [Fe(II)] versus time during pulse-feeding experiments. Oxidation rates were calculated by determining the slope of [Fe(II)] versus time when the Fe(II) concentrations were >100 μM.

added to a bioreactor. The bioreactor contained live cells when the first pulse was added. After the Fe(II) oxidation rate was measured, the cells were killed with sodium azide, and a second oxidation rate measurement was obtained. The difference in the rates represented the bacterial oxidation of Fe(II). As determined by this direct approach, bacterial oxidation accounted for 18 to 53% of the total Fe(II) oxidation (Table 2). When sodium azide was added to abiotically formed oxides, the Fe(II) oxidation rate decreased by 6%, and there was no change in the rate for consecutive measurements obtained with live cells (i.e., no sodium azide added) (data not shown). The variability in the Fe(II) oxidation rates between dates was primarily due to large differences in [Fe]_{total} in the bioreactors (e.g., <2 mM total Fe for the 20 February measurements versus 35 mM total Fe for the 9 May measurements). Dividing the bacterial oxidation rate (i.e., the difference between the rates before and after azide addition) by the cell population gave an average cell-specific Fe(II) oxidation rate of 4.2×10^{-2} pmol cell⁻¹ h⁻¹ [$n = 4$; range, 8.3×10^{-3} to 1.4×10^{-1} pmol of Fe(II) oxidized cell⁻¹ h⁻¹]. Using this average cell-specific Fe(II) oxidation rate and a calculated cell size of 1.2×10^{-14} g of C cell⁻¹, we calculated an average growth yield of 0.70 g of CH₂O per mol of Fe(II) oxidized [range, 0.21 to 3.5 g of CH₂O per mol of Fe(II)].

Oxidation rates in continuous-feeding mode. Because there were differences in the Fe(II) addition rate, [Fe]_{total}, and [Fe(II)] between bioreactors with and without live cells (Fig. 1), it was difficult to directly compare oxidation rates in paired

TABLE 2. Microbial contribution to total Fe(II) oxidation—direct measurement^a

Date	Fe(II) oxidation rate (μM h ⁻¹)		% Biotic
	Before azide addition	After azide addition	
20 February 2001	63	43	32
13 March 2001 ^b	81	59	27
28 March 2001	314	256	18
9 May 2001	885	414	53

^a Unless otherwise indicated, all data are for strain BrT. Biotic Fe(II) oxidation was measured directly by determining the difference between successive oxidation rate measurements in the same bioreactor. The first run contained live cells (before azide addition; biotic plus abiotic oxidation) and was followed by a run with killed cells (after azide addition; abiotic oxidation only).

^b Data for the marine Fe(II) oxidizer JV-1.

TABLE 1. Cell growth data for BrT

Inoculation date	Feeding mode	Doubling time (h)	Maximum cell density (cells ml ⁻¹)
13 December 2000	Pulse	33.3 ± 3.8	2.1×10^{6a}
16 January 2001	Pulse	22.9 ± 5.8	1.3×10^7
20 February 2001	Pulse	23.6 ± 7.9	9.8×10^6
28 March 2001	Continuous	30.5 ± 2.4 ^b	1.8×10^7
9 May 2001	Continuous	16.7 ± 3.0	1.4×10^7

^a The experiment was stopped before the stationary growth phase was reached.

^b Doubling time calculated for the period after the Fe(II) supply was restored.

TABLE 3. Multiple linear regression model parameters^a

Treatment	m_1	m_2	m_3	b	r^2
Live cells	10.47 (4.67)A	0.0020 (0.0007)B	0.843 (0.020)B	-20.46 (12.53)D	0.989
Killed cells	15.56 (4.95)A	0.0110 (0.0032)A	0.577 (0.097)A	-49.15 (14.47)A	0.919
No cells	15.30 (6.82)B	0.0026 (0.0013)C	0.700 (0.047)A	-11.91 (11.22)D	0.916

^a The Fe(II) oxidation rate (r) [micromolar Fe(II) oxidized per hour] is calculated as follows: $r = m_1 \times [\text{O}_2] + m_2 \times [\text{Fe}]_{\text{total}} + m_3 \times [\text{Fe(II) addition rate}] + b$, where the units for $[\text{O}_2]$ are the percentage of air saturation, the units for $[\text{Fe}]_{\text{total}}$ are micromolar, and the units for Fe(II) addition rate are micromolar per hour. The values in parentheses are standard deviations. Also shown is the regression coefficient for each model (r^2). The letters after the values indicate the significance of each term to the regression model, as follows: A, $P < 0.001$; B, $P < 0.01$; C, $P < 0.05$; D, not significant.

bioreactors. For example, the Fe(II) disappearance rate measured at ~189 h during the experimental run shown in Fig. 1 ranged from 216 $\mu\text{M h}^{-1}$ (abiotic oxides only) to 462 $\mu\text{M h}^{-1}$ (live cells plus oxides). While some of the difference may reflect bacterial Fe(II) metabolism (oxidation), $[\text{Fe}]_{\text{total}}$ was nearly twofold greater in the live-cell bioreactor. There were also differences in $[\text{Fe(II)}]$ and the Fe(II) addition rate (Fig. 1) that further confounded direct interpretation of the experimental data. Because there were very few cases where all conditions were similar in paired bioreactors, a modeling approach was required to analyze the continuous-feeding data and determine the contribution of Fe(II)-oxidizing bacteria to total Fe(II) oxidation.

The stepwise multiple linear regression analysis showed that the Fe(II) addition rate, $[\text{O}_2]$, and $[\text{Fe}]_{\text{total}}$ were significant components ($P < 0.05$) that contributed to the variation in the Fe(II) oxidation rate for all three treatments (live, killed, no cells). When these parameters were used, the regression coefficients (r^2) for the Fe(II) oxidation rates ranged from 0.92 to 0.99 (Table 3). Partial correlation analysis showed that within each treatment, more than 85% of the variance in the observed oxidation rates was due to the Fe(II) addition rate, whereas less than 3% was due to $[\text{O}_2]$ or $[\text{Fe}]_{\text{total}}$. Each of these variables was positively correlated with Fe(II) oxidation rates (Table 3). Other parameters, including $[\text{Fe(II)}]$ and $[\text{H}^+]$, were significant in some, but not all, treatments and were therefore not included in the final regression models. As mentioned above, cell density was not included as a parameter in the regression analysis due to the low number of samples for which both Fe(II) oxidation rates and cell density were measured. The model residuals were most variable at low Fe(II) addition rates (less than $\sim 50 \mu\text{M h}^{-1}$) but did not indicate systematic over- or underestimation of Fe(II) oxidation rates.

Fe(II) oxidation rates were calculated for live-, killed-, and no-cell treatments by using equation 1, the regression parameters presented in Table 3, and the following standard set of input conditions that were consistent with the experimental data: $[\text{O}_2]$, 0.5 or 3.0%; $[\text{Fe}]_{\text{total}}$, 1 or 10 mM; and Fe(II) addition rate, 100 to 600 $\mu\text{M h}^{-1}$. For example, the total Fe(II) oxidation rate for the live-cell treatment at an $[\text{O}_2]$ of 0.5%, an $[\text{Fe}]_{\text{total}}$ of 1,000 μM , and an Fe(II) addition rate of 300 $\mu\text{M h}^{-1}$ was calculated as follows: rate = $(10.47 \times 0.5) + (0.0020 \times 1,000) + (0.843 \times 300) - 20.46 = 240 \mu\text{M h}^{-1}$. The calculated mean oxidation rates for all input conditions and treatments ranged from 27 ± 14 to $537 \pm 19 \mu\text{M h}^{-1}$ (mean \pm standard deviation) (Fig. 4 and Table 4) and were generally comparable to those measured following the addition of Fe(II) pulses to the bioreactors (Table 2). Because the multiple linear regression models are statistical models, they should not be

used to extrapolate Fe(II) oxidation rates outside the range of the experimental conditions. For example, the models cannot forecast oxidation rates at O_2 concentrations that are <0.5 or $>5\%$ of air saturation.

The propagation of error terms in the regression models resulted in few significant differences between modeled oxida-

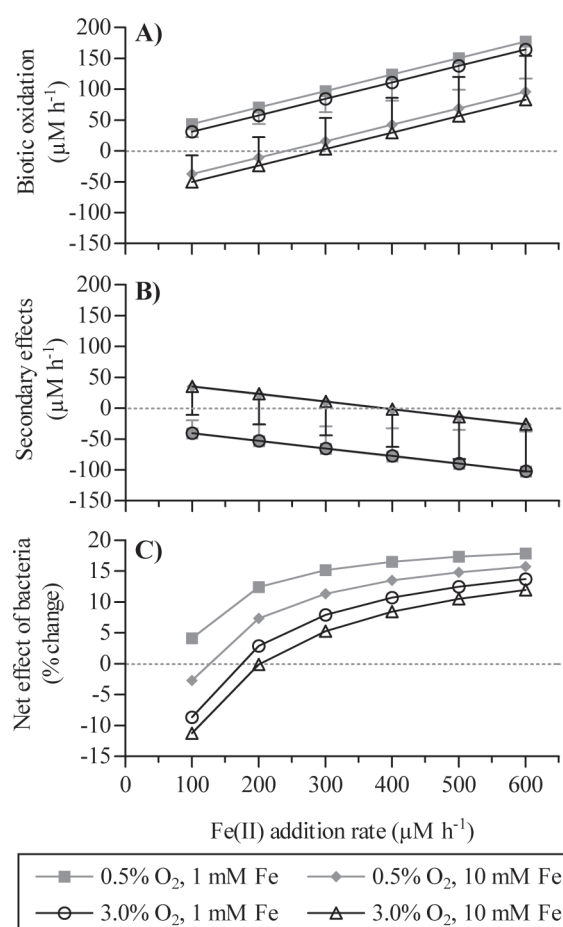


FIG. 4. Variations in modeled Fe(II) oxidation rates with changes in $[\text{O}_2]$, $[\text{Fe}]_{\text{total}}$, and the Fe(II) addition rate. For clarity, standard deviations are shown only for the model output obtained at 0.5% O_2 and 1 mM $[\text{Fe}]_{\text{total}}$ and at 3.0% O_2 and 10 mM $[\text{Fe}]_{\text{total}}$. (A) Biotic oxidation rates. (B) Secondary effects on abiotic oxidation rates. Negative values imply that the dead cells or cellular by-products inhibited chemical oxidation rates. (C) Net effect of cells on total Fe(II) oxidation rates, expressed as the percentage of change compared with the value for the no-cell treatment. Positive values indicate that the cells increased the total oxidation rate.

TABLE 4. Microbial contribution to total Fe(II) oxidation—statistical modeling^a

[O ₂] (% of air saturation)	[Fe] _{total} (mM)	Fe(II) addition rate (μM h ⁻¹)	Fe(II) oxidation rate (μM h ⁻¹)		% Biotic
			Total	Biotic	
0.5	1	100	71	44	62
		600	493	177	36
0.5	10	300 ^b	257	16	6
		600	511	96	19
3.0	1	100	97	31	32
		600	519	165	32
3.0	10	300 ^b	284	3	1
		600	537	83	16

^a Total and biotic Fe(II) oxidation rates were calculated as described in the text.

^b At Fe(II) addition rates of <300 μM h⁻¹, the modeled biotic oxidation rates with an [Fe]_{total} of 10 mM were negative; under these conditions, the biotic contribution to total Fe(II) oxidation could not be calculated.

tion rates. Therefore, general trends rather than statistical significance are discussed below. The biotic oxidation rates increased with increasing rates of Fe(II) addition and decreasing [Fe]_{total} (Fig. 4A), with the highest biotic oxidation rates occurring at low [O₂] and [Fe]_{total} and a high rate of Fe(II) addition. There was little difference in the modeled biotic oxidation rates over the range of O₂ saturation values. As indicated by the size of the error bars, most of the negative biotic oxidation rates in Fig. 4A are not significantly different from zero. When expressed as a percentage of total Fe(II) oxidation, biotic oxidation accounted for 1 to >60% of the total oxidation (median, 32%; *n* = 20) (Table 4).

Under all conditions when the [Fe]_{total} was low and when the [Fe]_{total} was high with a high Fe(II) addition rate, the modeled oxidation rates for the killed-cell treatment were depressed compared with the rates for the no-cell treatment (~20 to 40% depression at low [Fe]_{total}; <5% depression at high [Fe]_{total}), indicating that the dead bacterial cells inhibited abiotic oxidation under these conditions. In contrast, at a high [Fe]_{total} and a low Fe(II) addition rate, the oxidation rate was higher (generally by <20%) for the killed-cell treatment than for the no-cell treatment. As was the case for biotic oxidation, the degree of O₂ saturation did not influence the effects of dead cells on abiotic Fe(II) oxidation (Fig. 4B). The net result of the microbial metabolism of Fe(II) and the bacterial suppression of chemical Fe(II) oxidation rates was to (generally) increase total oxidation rates by up to 18% compared to the rates for the no-cell treatment (Fig. 4C). The live Fe(II) oxidizers had a greater effect at lower [O₂]. Similarly, the net effect of the bacteria was greater when [Fe]_{total} was 1 mM than when [Fe]_{total} was 10 mM.

DISCUSSION

Contribution of bacterial metabolism to Fe(II) oxidation. Two independent techniques (direct measurement and statistical modeling) provided evidence that strain BrT can significantly contribute to total Fe(II) oxidation rates under circumneutral conditions. As previously mentioned, bioreactors are unable to duplicate the complexity of the rhizosphere so caution must be used when the results are extrapolated to the

natural environment. Measurements of Fe(II) oxidation rates in a bioreactor with live cells, followed by azide addition and a subsequent rate measurement with the killed cells, provided direct evidence that this rhizosphere Fe(II) oxidizer can account for 18 to >50% of the total iron oxidation under circumneutral conditions (Table 2). Because there was only a small (6%) change in the oxidation rate for consecutive measurements with live cells and no change following the addition of azide to abiotic Fe(III) oxides with no cells, the large decrease in the rate following azide addition to live cells was not due to measurement variability or to azide effects on abiotic oxidation rates. A comparison of the modeled oxidation rates for the live- and killed-cell treatments provided a second method of estimating the bacterial contribution to total Fe oxidation. When this approach was used, biotic oxidation accounted for 32 to 62% of the total oxidation at a low [Fe]_{total} (1 mM) and up to 19% of the total oxidation at a high [Fe]_{total} (10 mM) (Table 4). The bacterial contribution was lower at the high [Fe]_{total} due to increased autocatalytic oxidation (see equation 2) and therefore greater competition for a limited Fe(II) supply. Together, these independent calculations indicate that strain BrT can mediate 20 to 50% of the total Fe(II) oxidation under circumneutral conditions.

The biotic fraction of total Fe(II) oxidation calculated in this study for strain BrT is at the low end of values reported previously for other circumneutral lithotrophic Fe(II) oxidizers. For example, Emerson and Revsbech (12) reported that addition of sodium azide to samples taken from a microbial mat at an iron seep depressed Fe(II) oxidation rates by 39%, whereas a comparison of Fe(II) oxidation rates in viable and pasteurized mat material indicated that microbial oxidation could account for 45 to 80% of the total oxidation. By comparing the Fe(III) deposition in a gradient system and that in a diffusion microprobe, Sobolev and Roden (28) calculated that a neutrophilic iron oxidizer from the sediments of a freshwater wetland was responsible for nearly 90% of the total Fe(III) oxide generated. As discussed below, the organism used in this study did not appear to show optimal growth in the bioreactors so the bacterial contribution to total Fe(II) oxidation reported here may underestimate the significance of this organism in the environment. In stark contrast to our findings and those cited above, van Bodegom et al. (35) reported that microbial Fe(II) oxidation was insignificant in soil from a rice paddy. However, the experimental manipulations of these authors, including the use of air-dried soil and shaking of soil slurries, may have preferentially favored abiotic Fe(II) oxidation and consequently underestimated the significance of microaerophilic Fe(II) oxidizers.

Cell growth. Strain BrT is an obligate lithotroph that is phylogenetically related to other Fe(II) oxidizers (10, 13; Weiss, unpublished data) and does not grow in the absence of an Fe(II) source. Under microaerophilic, circumneutral conditions in a bioreactor, strain BrT grew slowly, with doubling times of 16 to 33 h. These doubling times are ~1.5 to 2 times longer than those measured for BrT growth in gel-stabilized gradient tubes (15 to 20 h) (Weiss, unpublished data) and are 2 to 4 times longer than those measured for the phylogenetically similar strains ES-1 and ES-2 (8 to 12.5 h) (10). Furthermore, the maximum cell densities in the bioreactor were approximately one-half of those in gradient tubes (Weiss,

unpublished data). Our calculated growth yield of 0.70 g of CH_2O per mol of Fe(II) oxidized is equivalent to 0.28 mol of biomass C per mol of Fe(II) oxidized. This growth yield is similar to the yields of 0.17 to 0.29 mol of C per mol of Fe(II) calculated for lithotrophic Fe(II) oxidizers in opposing gradient systems (27).

The combination of longer doubling times and lower maximum cell densities in the bioreactors than in gradient systems suggests that a well-mixed bioreactor was not the optimal system for an organism that typically grows in a diffusive boundary zone. One possible explanation is that the organism cannot deal with the stresses associated with a rapidly stirred system. A second hypothesis is that the Fe(II) oxidizers become Fe(II) limited in a bioreactor due to autocatalysis by Fe(III) oxides. In contrast, Fe(II) oxidizers in an attached flowthrough or gradient system may be able to position themselves so that cellular contact with Fe(II) is maximized while exposure of Fe(III) oxides to the flux of Fe(II) is minimized. Regardless of the mechanism, the microbial Fe(II) oxidation rates reported for strain BrT in this study may underestimate the actual rates in the more stable, diffusively driven rhizosphere.

Bacterial effects on abiotic Fe(II) oxidation. Based on a comparison of the modeled oxidation rates for the killed-cell and no-cell treatments (Fig 4B), it appears that strain BrT inhibits abiotic iron oxidation. This effect is distinct from competition for Fe(II) or O_2 between live cells and abiotic oxides as the inhibition was observed after the cells were killed. One hypothesis is that exopolymers or other organic extracellular molecules produced by the bacteria bind dissolved Fe(II) and make it less available for chemical oxidation. Theis and Singer (33) proposed that organic matter could affect chemical Fe(II) oxidation rates by binding to free Fe(II). Depending on the stability constant of the Fe(II)-organic matter complex (33), the concentrations of organic matter, O_2 , and Fe(II) (19), and the nature of the organic matter (24, 30, 33), organic matter can either inhibit, accelerate, or have no effect on abiotic Fe(II) oxidation. For example, the inhibition of chemical oxidation rates by bacterial exopolysaccharides was also proposed as a mechanism to explain higher rates of Fe plaque (oxide) formation on axenic rice (*Oryza sativa*) roots than on nonaxenic rice roots (18). Strain BrT does produce an extracellular organic matrix (J. V. Weiss, personal communication), but this matrix has not been characterized yet. An organic matrix has been reported for the phylogenetically similar strains ES-1 and ES-2 (10), and it has been proposed that this matrix may prevent the cells from becoming entrapped in the insoluble Fe(III) oxides that result from their metabolism. Furthermore, Sobolev and Roden (28) have suggested that another circumneutral Fe(II) oxidizer (strain TW2) produces organic compounds that maintain Fe(III) in a soluble or colloidal state. We amend these proposals and suggest that exopolymer matrices can temporarily bind Fe(II), thus making it less available for chemical oxidation. This may be an additional evolutionary strategy developed by the organisms in order to compete with rapid rates of abiotic Fe(II) oxidation in circumneutral environments.

Abiotic effects on total Fe(II) oxidation. In dynamic systems, such as the continuously fed bioreactors and the natural environment, the instantaneous Fe(II) concentration is actually the net result of Fe(II) delivery and removal by oxidation and does

not accurately reflect the total Fe(II) available for oxidation. Instead of using existing models (e.g., equation 2) (31, 32) that rely on [Fe(II)] as an input term, multiple linear regression analyses were conducted to identify the variables that control Fe(II) oxidation rates. For each treatment (live, killed, and no cells), the Fe(II) addition rate, $[\text{O}_2]$, and $[\text{Fe}]_{\text{total}}$ were significant components of the regression and were positively correlated with the Fe(II) oxidation rate. Partial correlation analysis indicated that the Fe(II) addition rate explained 88% (killed-cell treatment) to 98% (live cells) of the variability in oxidation rates, with $[\text{O}_2]$ and $[\text{Fe}]_{\text{total}}$ each accounting for less than 3% of the variability. The strong dependence of oxidation rate on the Fe(II) addition rate, coupled with the lack of significant Fe(II) accumulation in the bioreactors (Fig. 1C), suggests that the bioreactors were highly Fe(II) limited. Even at high Fe(II) addition rates ($>600 \mu\text{M h}^{-1}$), $89\% \pm 4\%$ (average \pm standard deviation; $n = 6$) of the added Fe(II) was oxidized over the time scale of the measurement (~ 30 to 60 min). The growth of the Fe(II) oxidizers indicates that the bacteria successfully competed with abiotic oxidation for Fe(II), despite the Fe(II) limitation in the bioreactor. This observation raises the important point that Fe(II) limitation of total system oxidation does not necessarily signify Fe(II) limitation of microbial Fe(II) oxidation.

Environmental relevance. The growth conditions and input parameters for the statistical models, including pH, $[\text{O}_2]$, and Fe(II) addition rates, approximate conditions observed in the rhizosphere in a range of field and lab studies. The relatively low oxygen concentrations used in this study (0.5 to 3% of air saturation or ~ 2 to $9 \mu\text{M}$) fall within the reported range of O_2 concentrations in the rhizosphere (0 to $150 \mu\text{M}$) (reference 34 and references therein) and are consistent with reports that circumneutral lithotrophic Fe(II) oxidizers prefer microaerophilic conditions (10, 28). The pH used in this study ($\text{pH } 6.5 \pm 0.1$) is at the upper range of porewater pH values ($\text{pH } 3.7$ to 6.8) in 13 wetland and aquatic environments where lithotrophic Fe(II) oxidizers were identified (Weiss et al., submitted). As a first approximation of Fe(II) delivery rates in a natural wetland, we used a dissolved Fe(II) profile from a *J. effusus* (soft rush)-dominated wetland in the southeastern United States (23). Using Fick's first law of diffusion, an Fe(II) diffusion coefficient of $0.7 \text{ cm}^2 \text{ day}^{-1}$, and an Fe(II) concentration gradient of $0.46 \mu\text{mol cm}^{-4}$ (at depths of ~ 16 to 26 cm) (23), we estimated an Fe(II) flux into the rhizosphere of $0.32 \mu\text{mol of Fe(II) cm}^{-2} \text{ day}^{-1}$. Assuming that Fe(II) oxidation occurs within 0.25 to 1 mm of an oxic-anoxic boundary (e.g., the root-sediment interface), this vertical flux is equivalent to a volumetric flux of 134 to $537 \mu\text{M h}^{-1}$. This range overlaps the Fe(II) addition rates (100 to $600 \mu\text{M h}^{-1}$) used as input terms in our statistical model. Low Fe(II) concentrations in the root zone in natural wetlands and experimental cores (2, 23; Weiss, unpublished data) indicate that Fe(II) oxidation is tightly coupled to the delivery of Fe(II) to the root surface via local reduction of Fe(III) oxides or diffusion from outside the root zone and suggest that the Fe(II)-limited conditions in a bioreactor may be representative of the natural environment.

Although other researchers have suggested that iron bacteria enhance abiotic Fe oxidation by serving as surfaces that promote abiotic oxidation (29), our results demonstrate that strain BrT actively metabolizes Fe(II) and can account for a

maximum of 50 to 60% of the total Fe(II) oxidation in laboratory cultures. Because the data suggest that optimal growth of this Fe(II) oxidizer was not obtained in a bioreactor, microbial Fe(II) oxidation may be even more important in the natural environment. Since Fe(II) oxidation can be the dominant O₂-consuming process in the rhizosphere (34) and circumneutral Fe(II) oxidizers can accelerate total Fe(II) oxidation rates (this study), the activity of these organisms may reduce the amount of O₂ available to drive other O₂-consuming reactions. Changes in O₂ availability and coupling between Fe(II) oxidation and Fe(III) reduction in a localized iron cycle (23) can influence the biogeochemistry of other elements, including carbon, phosphorus, and sulfur (4, 15, 23).

ACKNOWLEDGMENTS

We thank Chris Bradburne for laboratory assistance with the bioreactors, especially during the early phases of this research. We also thank Johanna Weiss for providing the pure rhizosphere cultures used in this research and unpublished data on the growth characteristics of strain BrT. Finally, we thank Eric Roden for his help with calculating wetland Fe(II) diffusion rates and Eric Roden and an anonymous reviewer for their constructive comments on the manuscript.

This work was supported in part by NSF grant DEB-9986981 to J.P.M. and D.E., as well as by NSF grant MCB-9723459 and a NASA Astrobiology Award to D.E.

REFERENCES

1. **Armstrong, W.** 1964. Oxygen diffusion from the roots of some British bog plants. *Nature* **204**:801–802.
2. **Begg, C. B. M., G. J. D. Kirk, A. F. MacKenzie, and H.-U. Neue.** 1994. Root-induced iron oxidation and pH changes in the lowland rice rhizosphere. *New Phytol.* **128**:469–477.
3. **Brix, H.** 1993. Macrophyte-mediated oxygen transfer in wetlands: transport mechanisms and rates, p. 391–398. *In* G. Moshiri (ed.), *Constructed wetlands for water quality improvement*. CRC Press, Boca Raton, Fla.
4. **Chambers, R. M., and W. E. Odum.** 1990. Porewater oxidation, dissolved phosphate and the iron curtain: iron-phosphorus relations in tidal freshwater marshes. *Biogeochemistry* **10**:37–52.
5. **Dymond, J., R. W. Collier, and M. E. Watwood.** 1989. Bacterial mats from Crater Lake, Oregon and their relationship to possible deep-lake hydrothermal venting. *Nature* **342**:673–675.
6. **Ehrenberg, C. G.** 1838. *Gallionella ferruginea*. Taylor's Sci. Mem. **1**:402.
7. **Ehrlich, H. L., W. J. Ingledew, and J. C. Salerno.** 1991. Iron- and manganese-oxidizing bacteria, p. 147–170. *In* J. M. Shively and L. L. Barton (ed.), *Variations in autotrophic life*. Academic Press, San Diego, Calif.
8. **Emerson, D.** 2000. Microbial oxidation of Fe(II) and Mn(II) at circumneutral pH, p. 31–52. *In* D. R. Lovley (ed.), *Environmental microbe-metal interactions*. American Society for Microbiology, Washington, D.C.
9. **Emerson, D., and C. L. Moyer.** 2002. Neutrophilic Fe-oxidizing bacteria are abundant at the Loihi Seamount hydrothermal vents and play a major role in Fe oxide deposition. *Appl. Environ. Microbiol.* **68**:3085–3093.
10. **Emerson, D., and C. L. Moyer.** 1997. Isolation and characterization of novel iron-oxidizing bacteria that grow at circumneutral pH. *Appl. Environ. Microbiol.* **63**:4784–4792.
11. **Emerson, D., and N. P. Revsbech.** 1994. Investigation of an iron-oxidizing microbial mat community located near Aarhus, Denmark: field studies. *Appl. Environ. Microbiol.* **60**:4022–4031.
12. **Emerson, D., and N. P. Revsbech.** 1994. Investigation of an iron-oxidizing microbial mat community located near Aarhus, Denmark: laboratory studies. *Appl. Environ. Microbiol.* **60**:4032–4038.
13. **Emerson, D., J. V. Weiss, and J. P. Megonigal.** 1999. Iron-oxidizing bacteria are associated with ferric hydroxide precipitate (Fe plaque) on the roots of wetland plants. *Appl. Environ. Microbiol.* **65**:2758–2761.
14. **Ghiorse, W. C., and H. L. Ehrlich.** 1993. Microbial biomineralization of iron and manganese, p. 75–107. *In* R. W. Fitzpatrick and H. C. W. Skinner (ed.), *Iron and manganese biomineralization processes in modern and ancient environments*. Catena, Cremlingen-Destedt, Germany.
15. **Giblin, A. E., and R. W. Howarth.** 1984. Porewater evidence for a dynamic sedimentary iron cycle in salt marshes. *Limnol. Oceanogr.* **29**:47–63.
16. **Hallbeck, L., and K. Pederson.** 1991. Autotrophic and mixotrophic growth of *Gallionella ferruginea*. *J. Gen. Microbiol.* **137**:2657–2661.
17. **Jannasch, H. W., and M. J. Mottl.** 1985. Geomicrobiology of deep-sea hydrothermal vents. *Science* **229**:717–725.
18. **Johnson-Green, P. C., and A. A. Crowder.** 1991. Iron oxide deposition on axenic and non-axenic roots of rice seedlings (*Oryza sativa* L.). *J. Plant Nutr.* **14**:375–386.
19. **Liang, L., J. A. McNabb, J. M. Paulk, B. Gu, and J. F. McCarthy.** 1993. Kinetics of Fe(II) oxygenation at low partial pressure of oxygen in the presence of natural organic matter. *Environ. Sci. Technol.* **27**:1864–1870.
20. **Lovley, D. R., and E. J. P. Phillips.** 1986. Availability of ferric iron for microbial reduction in bottom sediments of the freshwater tidal Potomac River. *Appl. Environ. Microbiol.* **52**:751–757.
21. **Mendelsohn, I. A., B. A. Kleiss, and J. S. Wakeley.** 1995. Factors controlling the formation of oxidized root channels: a review. *Wetlands* **15**:37–46.
22. **Mulder, E. G., and M. H. Deinema.** 1992. The sheathed bacteria, p. 2612–2624. *In* H. G. Trüper, A. Balows, M. Dworkin, W. Harder, and K. H. Schleifer (ed.), *The prokaryotes*, vol. 2. Springer-Verlag, New York, N.Y.
23. **Roden, E. E., and R. G. Wetzel.** 1996. Organic carbon oxidation and suppression of methane production by microbial Fe(III) oxide reduction in vegetated and unvegetated freshwater wetland sediments. *Limnol. Oceanogr.* **41**:1733–1748.
24. **Roth, R. I., S. S. Panter, A. I. Zegna, and J. Levin.** 2000. Bacterial endotoxin (lipopolysaccharide) stimulates the rate of iron oxidation. *J. Endotoxin Res.* **6**:313–319.
25. **Singer, P. C., and W. Stumm.** 1970. Acidic mine drainage: the rate-determining step. *Science* **167**:1121–1123.
26. **Skoog, D. A., and D. M. West.** 1963. *Fundamentals of analytical chemistry*, 3rd ed., p. 71–78. Holt, Rinehart, and Winston, New York, N.Y.
27. **Sobolev, D.** 2001. Isolation and characterization of a neutrophilic Fe(II)-oxidizing bacterium and assessment of the potential for rapid Fe redox cycling at the aerobic-anaerobic interface. Ph.D. dissertation. University of Alabama, Tuscaloosa.
28. **Sobolev, D., and E. E. Roden.** 2001. Suboxic deposition of ferric iron by bacteria in opposing gradients of Fe(II) and oxygen at circumneutral pH. *Appl. Environ. Microbiol.* **67**:1328–1334.
29. **St.-Cyr, L., D. Fortin, and P. G. C. Campbell.** 1993. Microscopic observations of the iron plaque of a submerged aquatic plant (*Vallisneria spiralis* Michx.). *Aquat. Bot.* **46**:155–167.
30. **Stone, A. T.** 1997. Reactions of extracellular organic ligands with dissolved metal ions and mineral surfaces, p. 309–344. *In* J. Banfield and K. H. Nealson (ed.), *Geomicrobiology: interaction between microbes and minerals*. Mineralogical Society of America, Washington, D.C.
31. **Stumm, W., and J. J. Morgan.** 1981. *Aquatic chemistry: an introduction emphasizing chemical equilibria in natural waters*, 2nd ed. Wiley-Interscience, New York, N.Y.
32. **Sung, W., and J. J. Morgan.** 1980. Kinetics and product of ferrous iron oxygenation in aqueous systems. *Environ. Sci. Technol.* **14**:561–568.
33. **Theis, T. L., and P. C. Singer.** 1974. Complexation of iron(II) by organic matter and its effect on iron(II) oxygenation. *Environ. Sci. Technol.* **8**:569–573.
34. **van Bodegom, P., J. Goudriaan, and P. Leffelaar.** 2001. A mechanistic model of methane oxidation in a rice rhizosphere. *Biogeochemistry* **55**:145–177.
35. **van Bodegom, P., F. Stams, L. Mollema, S. Boeke, and P. Leffelaar.** 2001. Methane oxidation and the competition for oxygen in the rice rhizosphere. *Appl. Environ. Microbiol.* **67**:3586–3597.